Constitutive Modeling of Geologic Media and Joints, and Application of Numerical Methods

Chandrakant S. Desai

Abstract

Appropriate modeling of the behavior of engineering materials and joints (or interfaces) is vital for realistic solutions from both conventional (analytical) and modern computer (finite element) methods. In other words, consistent material or constitutive models based on the fundamental principles of mechanics, testing of specimens in the laboratory (and field), and validations with respect to the behavior in the laboratory and field (prototype), are essential for development of realistic and dependable procedures for design and analysis.

In the case of utilization of underground space, it is required to develop realistic constitutive models for materials such as soil, rock and coal, including discontinuities such as joints. Now a days, numerical methods have been often used for solution of underground space problems requiring analysis, design, construction, and maintenance.

This paper emphasizes basic, laboratory and validation aspects in the development of constitutive models. Here a recently developed unified modeling approach called Disturbed State Concept (DSC), which allows, in the same mathematical framework, various behavioral features such as elastic, plastic and creep strains, stress path, volume change, continuous yielding, microcracking leading to softening and fracture, healing or strengthening and different types loadings including environmental such as thermal and fluids.

The DSC models have been implemented in computer (finite element) procedures for multidimensional analysis. Typical solutions of boundary value (practical) problems including validation with respect to laboratory and field measurements are presented here, and the importance of appropriate and realistic constitutive models is emphasized.

Constitutive Models

A geologic material with joints is affected by a number of factors such as (1) state of stress or strain, (2) stress path, (3) volume change, (4) irreversible or plastic deformation, (5) continuous yielding, (6) creep, (7) microcracking leading to softening and failure, (8) temperature, (9) type of loading such as static, cyclic, repetitive and dynamic, and (10) rate of loading. Materials and joints in underground space are influenced by many of the factors listed here. A constitutive model for a material should be based on basic principles that take into account effects of these factors, as well as validated with respect to measured behavior of relevant practical problems. Details of the constitutive models and the DSC are presented by Desai (2001).

Conventional constitutive models such as elasticity (linear and nonlinear), and plasticity do not handle most of the factors stated above. The continuous yield models such as critical state, Roscoe, et al. (1958), and Cap, DiMaggio and Sandler (1971), represent improvement over classical plasticity models, particularly since they allow for important issue of continuous yielding. The Hierarchical Single Surface (HISS) plasticity model (Desai, 2001; Desai et al. 1986) provides significant improvements over the classical and continuous yield models; it

Department of Civil Engineering and Engineering Mechanics
The University of Arizona
Tucson, AZ, USA 85721-0072

allows for state of stress, stress path, volume change, elastic, plastic and creep deformations, and continuous yielding. One of the important advantages of the HISS model is that it is general and unified, and includes almost all previous plasticity models as special cases (Desai, 2001).

The above models are based on the theories of continuum mechanics. Hence, it is assumed that the material is continuous before and after the loadings. However, many geologic materials and joints contain (microstructural) discontinuities initially, and they grow and/or form during the loading. Hence, a material model that allows for the effect of the initiation and growth of discontinuities, which are often considered due to microcracking leading to softening, fracture and failure, is needed.

Micromechanical methods fracture and damage models have been proposed to allow for the discontinuities (Desai, 2001; Muhlhaus, 1995). However, they may suffer from limitations such as lack of appropriate tests at the micro level to develop constitutive models, and spurious mesh dependence in computer procedures.

The Disturbed State Concept (DSC) does not depend on micro level constitutive models and does not cause spurious mesh dependence. It is general and unified, and many available models are considered to be its special cases.

Disturbed State Concept (DSC)

The DSC modeling approach has been developed based on significant attention to the interplay of basic mechanics and comprehensive (laboratory) testing. The DSC provides a general and unified procedure to develop constitutive models for solid (geologic, concrete, asphalt concrete, metals, alloys, etc.) and interfaces and joints in structures and rock masses, (Desai, 2001; Desai and Ma, 1992; Desai and Toth, 1996; Desai et al. 1984). A main attribute of the procedure is that it has a unified basis of mechanics from which many other available models can be obtained as special cases. Moreover, the general framework allows modeling of both solids and discontinuities (interfaces and joints), and allows use of continuum theories (elasticity, plasticity, etc.) and disturbance that causes microcracking or healing.

In the DSC, a loaded or unloaded material is considered to be composed of two or more phases. For instance, a solid material element is assumed to be composed of a continuum phase (relative intact, RI), and disturbed or microcracked phase, which can approach an asymptotic state called the fully adjusted (FA) phase, Fig. 1. If the material is continuum (intact) initially, it is completely in the RI State. During loading, the RI phase transforms, and the FA phase is initiated and grows. The coupling or interaction between the RI and FA phase, is expressed through the disturbance function (D), which is a vital aspect of the DSC. For initial RI phase, D is 0, which increases during loading and approaches unity in the FA state, Fig. 2(a). The FA phase represents the ultimate state in the behavior of the material, Fig. 2(b).

DSC Equations

Based on equilibrium of forces acting on the two phase material, Fig. 1, the DSC equations can be derived as (1)

$$d\underset{\sim}{\sigma}^{a} = (1-D)\,d\underset{\sim}{\sigma}^{i} + D\,d\underset{\sim}{\sigma}^{c} + dD\left(\underset{\sim}{\sigma}^{c} - \underset{\sim}{\sigma}^{i}\right) \quad (1a)$$

where a, i, c denote behavior of the observed, relative intact and fully adjusted phases, respectively, dD denotes the increment or rate of D and underscore denotes vector and matrix. Substitution for the incremental constitutive models for the RI and FA phases leads to

$$d\underset{\sim}{a}^{a} = (1-D)\underset{\sim}{C}^{i}\,d\underset{\sim}{\varepsilon}^{i} + D\underset{\sim}{C}^{c}\,d\varepsilon^{c} + dD\left(\underset{\sim}{\sigma}^{c} - \underset{\sim}{\sigma}^{i}\right) \quad (1b)$$

where $\underset{\sim}{C}^{i}$ and $\underset{\sim}{C}^{c}$ are the constitutive matrices for the RI and FA phases, respectively.

We now need to define the constitutive behavior for the RI and FA phases and the disturbance, D.

Relative Intact

The material in the RI phase is considered to be continuous. Hence, appropriate theory, elasticity, plasticity, viscoplasticity, etc. can be used to define it. Accordingly, the constitutive relation for RI phase is given by

$$d\underset{\sim}{\sigma}^i = \underset{\sim}{C}^i \, d\underset{\sim}{\varepsilon}^i \quad (2)$$

where $\underset{\sim}{C}^i$ can be elastic, plastic, or elastoviscoplastic matrix. For linear elastic isotropic material, $\underset{\sim}{C}^i$ is composed of modulus of elasticity, E, and Poisson's ratio, . For elastoplasticity, we need to use a yield function and flow rule to derive

$$d\underset{\sim}{\sigma}^i = \left(\underset{\sim}{C}^e - \underset{\sim}{C}^p\right) d\underset{\sim}{\varepsilon}^i \quad (3)$$

where $\underset{\sim}{C}^p$ is the plasticity part of $\underset{\sim}{C}^i$, which can be derived by using classical plasticity (e.g., von Mises, Drucker-Prager, Mohr Coulomb) or continuous yield (critical state, Cap, etc.) models. We have proposed a general yield function that provides for capabilities to address factors beyond that are covered by the foregoing models. It is called the Hierarchical Single Surface (HISS) yield function. Most of the previously available models can be derived as special cases of HISS (Desai, 2001; Desai et al. 1986).

Hierarchical Single Surface (HISS) Plasticity

The yield function, according to HISS plasticity, is given by

$$F = \bar{J}_{2D} - \left(-\alpha \bar{J}_1^n + \gamma \bar{J}_1^2\right)\left(1 - \beta S_r\right)^{-0.50} = 0 \quad (4)$$

where $\bar{J}_{2D} = J_{2D} / p_a^2$, J_{2D} = second invariant of the deviatoric stress tensor, pa = atmospheric pressure constant, $\bar{J}_1 = (J_1 + 3R)/p_a$, J_1 = first invariant of the total stress tensor, R = term to include cohesive intercept $\bar{c}$, Fig. 3(a), n = parameter associated with the transition from compressive to dilative behavior, γ = parameter related to the ultimate yield, β related to the shape F in the 1- 2- 3 $\sigma_1 - \sigma_2 - \sigma_3$ space, Fig. 3(b), and α = growth or yielding or hardening function; a simple form is given by

$$\alpha = \frac{a_1}{\xi^{\eta_1}} \quad (5)$$

where a1 and η_1 = hardening parameters, and ξ = trajectory or accumulated plastic strains (or work) expressed as sum of deviatoric (ξ_D) and volumetric (ξ_v) plastic strain trajectories:

$$\xi = \xi_D + \xi_v = \int \left(dE_{ij}^p dE_{ij}^p\right)^{1/2} + \frac{1}{\sqrt{3}}\left|\varepsilon_{ii}^p\right| \quad (6)$$

where E_{ij}^p = deviatoric plastic strains tensor = $\varepsilon_{ij}^p - \frac{1}{3}\varepsilon^p{}_{ii}\delta_{ii}$, $\varepsilon_{ii}^p = \varepsilon_v^p$ = volumetric plastic strain.

The HISS yield surface can be modified for associated and nonassociated plasticity and anisotropic behavior (Somasundaram and Desai, 1988; Desai and Hashemi 1989). Here, only the associated plasticity is used with the DSC. However, the introduction of the disturbance (D) in the formulations allow for (a part of) the nonassociative behavior, in that it includes deviation from normality which is related to the nonassociative behavior.

Fully Adjusted Phase

The material in the ultimate or fully adjusted state can be assumed to possess no strength, strength like a constrained liquid, or strength like a liquid-solid. The assumption of no strength is a part of the classical damage model (Kachanov, 1986); because it ignores the coupling between the RI and FA states, it suffers from certain difficulties such as spurious mesh dependence, hence, it is not recommended. The assumption of constrained liquid is like in the classical plasticity and possesses bulk strength, defined by bulk modulus, K. The liquid-solid assumption is similar to the critical state model (Desai, 2001; Roscoe et al. 1958). The critical state is reached when under a given (initial) mean pressure, the volume of the material does change after a certain critical shear loading. According to the critical state, the strength in that state can be defined by the following two equations (Desai, 2001; Roscoe et al. 1958):

$$\sqrt{J_{2D}} = \overline{m} J_1 \quad (7a)$$

$$e^c = e_0^c - \lambda \ell n \left(J_1^c / 3 p_a \right) \quad (7b)$$

where $\overline{m}$, λ and e_0^c are the critical state parameters.

Disturbance

The disturbance (D) can be defined on the basis of observed behavior in terms stress and strain, volumetric strains, pore water pressure, and nondestructive behavior such as shear wave velocity. In terms of stress, it can be defined as (Fig. 2b):

$$D = \frac{\sigma^i - \sigma^a}{\sigma^i - \sigma^c} \quad (8a)$$

where σ^a is the measured stress. In the mathematical form, D can be expressed as

$$D = D_u \left[\left(1 - \exp(-A \xi_D^Z) \right) \right] \quad (8b)$$

where A and Z are parameters, D_u ultimate disturbance and ξ_D is the deviatoric plastic strain trajectory.

When the HISS plasticity for the RI Behavior is used, the constitutive equation can be expressed as

$$d\underset{\sim}{\sigma}^a = (1 - D) \underset{\sim}{C}^{ep} d\underset{\sim}{\varepsilon}^i + D \underset{\sim}{C}^c d\underset{\sim}{\varepsilon}^c + dD \left(\underset{\sim}{\sigma}^c - \underset{\sim}{\sigma}^i \right) \quad (9)$$

where $\underset{\sim}{C}^{ep}$ is derived by using the yield function F in Eq. (4).

Creep Behavior

Creep behavior can be important for materials in underground space. It can be incorporated in the DSC model. A procedure called Multicomponent DSC (MDSC) has been developed to handle various creep models such as viscoelastic (ve), elastoviscoplastic (evp) and viscoelastic viscoplastic (vevp); details of the models and applications are given in Desai (2001).

Thermal and Rate Effects

The DSC model has been extended to include the effects due to temperature and rate of loading (Desai, 2001; Desai et al. 1997; Desai et al. 2009).

Joints and Interfaces

Discontinuities in geologic media, e.g., rocks occur usually as joints, which can have significant influence on the behavior of engineering systems such as underground works. Depending upon the geometry, conditions of a joint, e.g., filled with gauge, and the properties of the adjoining rocks, the mechanism of deformation of joints can be different from that of the solid media (intact rock). Often there occurs relative motions at the joint, such as slip, debonding, rebonding and interpenetration. Hence, special consideration needs to be given to modeling and testing of joints. The model for joints by Goomen, et al. (1968) as the "zero" thickness element, has been often used. However, it

may suffer from certain difficulties such as instability for computation of normal stresses. The "thin-layer" element proposed by Desai, et al. (1984) is based on the idea that the joint element can be treated and formulated as the surrounding "solid" elements; however, its constitutive relation is derived from special (shear) tests in which shear and normal behavior can be measured (Desai, 2001; Desai et al., 1984).

When a problem involves, say, "solid" materials and joints, their deformation mechanism can be different; however, the form of their constitutive behavior should be similar. For instance, it may not be realistic to model a rock by elastoplastic continuous yield plasticity, while a joint as linear elastic. One of the major attributes of the DSC is that the model for a joint can be obtained from the DSC, by specializing the framework, Eq. (1). The yield surface for a joint, as the RI phase in the DSC, can be expressed, for the two-dimensional case, as

$$F = \tau^2 + \alpha\, \sigma_n^{*n} - \gamma\, \sigma_n^{*2} \quad (10)$$

where $\sigma_n^* = \sigma_n + R$, R = intercept along -ve σ_n (Fig. 4) and is related to the adhesion, c_0, n and γ are the phase change and ultimate parameters, and α is the hardening or yielding growth function:

$$\alpha = \frac{a}{\xi^b} \quad (11)$$

which has similar form as Eq. (5) for "solid," a and b are hardening parameters and ξ is the trajectory of or accumulated irreversible or plastic shear and normal relative displacements (Desai and Ma, 1992). The incremental constitutive equations for joints are given by

$$d\tau^a = (1-D)\,d\tau^i + D\,d\tau^c + dD\left(\tau^c - \tau^i\right) \quad (12a)$$

$$d\sigma_n^a = (1-D)\,d\sigma_n^i + D\,d\sigma_n^c + dD\left(\sigma_n^c - \sigma_n^i\right) \quad (12b)$$

Further details of the DSC for joints and interfaces are given in Desai (2001).

Validations

It is important to validate a proposed constitutive model. Validations can be performed at various levels: (1) Level 1 - Laboratory Specimen: Here the validations are obtained by comparing model predictions with the test data from which the (average) parameters were obtained, (2) Level 2 - Laboratory Specimen: The model predictions are compared with independent set of test data by using parameters determined from another set of test data, and (3) Level 3 - Boundary Value Problem: Here, the predictions from solution (finite element) procedure in which the constitutive model is implemented, are compared with measurements of practical problems in the field and/or simulated in the laboratory.

The DSC model has been implemented in two- and three-dimensional, static and dynamic finite element procedures. It has been validated for the three levels, for a wide range of materials, interfaces and joints, e.g., clays, sands, rocks, concrete, asphalt concrete, metals, alloys and silicon (Desai, 2001). Validations have also been obtained for interfaces in building-foundations, and joints in rock and concrete.

In view of the length of the paper, only typical validations at the specimen and practical problem levels are included herein. They include behavior of rocks and analysis of an underground powerhouse cavern.

Two- and Three-Dimensional FE procedures with the DSC constitutive model has been applied for solution of wide range of engineering problems such as geomechanical including underground systems, , structural dynamics, earthquake engineering, fluid flow through porous media, pavements, composites in electronic packaging and motion of glaciers and ice sheets (Desai, 2001; Desai et al., 2009). Details of constitutive modeling of rocks, joints in rocks

and solution of a practical underground space problem relevant to the theme of this conference, are given below.

Example 1: DSC Modeling of Rocks

A comprehensive research was performed to analyze the behavior of an underground cavern in the Nathpa-Jhakri hydropower project in the Himalayas; the descriptions herein are adopted from (Varadarajan et al., 2001a; 2001b); site plan is shown in Fig. 5. The rocks at the site include mainly three types: quartz mica schist (R1), quartz mica schist with quartz veins (R2) and biotite schist (R3). The properties of rocks are given in Table 1.

Table 1: Properties of Rocks

Type of Rock	Specific Gravity, G	Dry Density KN/m^3	Tensile Strength MPa
1. Quartz Mica Schist	2.74	26.0 – 27.6	8.00
2. Quartz Mica Schist with Qartz veins	2.83	26.0 – 27.4	10.00
3. Biotite Schist	2.82	26.4 – 27.9	6.00

Laboratory testing for the rocks was performed using the triaxial device under high pressure. Rock specimens of about 5.475 cm diameter and 10.95 cm length were tested under a number of initial confining pressures, 3 = 0 to 45 MPa. Test data for the three rocks under typical confining stress, are shown in Fig. 6 for quartz mica schist, Fig. 7 for quartz mica schist with quartz veins, and Fig. 8 for biotite schist.

The DSC model was used to characterize the behavior of rocks. The material parameters for the rocks are given in Table 2 & 3. Figures 6 to 8 also shows the predictions by the DSC. The predictions were obtained by two methods: (1) integration of Eq. (1) starting from the initial confining pressure, called single joint method (SPM), and (2) using the FEM with the DSC model. The finite element analyses were performed by discretizing the quarter of the test specimen, Fig. 9. It can be seen that the DSC model provides highly satisfactory correlation between the predictions and laboratory measurements (Table 4).

Example 2: DSC Modeling of Joints

The DSC model, depicted in Fig. 10, was applied for various joints and interfaces (Desai and Ma, 1992). Typical examples are presented below.

A series of laboratory tests, Types C, A and B, were performed by Schneider (1976). Type C limestone joint, represents smooth, Type A, granite joint, represents medium rough, and type B, sandstone joint, represents rough joint surfaces. The model constants were determined from the tests given in (Desai and Ma, 1992).

The predictions of the test behavior were obtained by integrating the incremental Eqs. (12). Figures 11(a), (c) and (e) show comparisons between predictions and test data for shear stress ( ) vs. relative shear displacement (u) for types C, A and B joints, respectively. In Figs. 11(b), (d) and (f) are shown the relative normal (v) vs. shear displacement (u) for (initial) normal stress, n = 0.61; = 1.38; and = 1.29 MPa, respectively. It can be seen from Fig. 11 that DSC results provide excellent correlation with measurements.

Example 3: Practical Problem - Powerhouse avern at Nathpa-Jhakri Hydropower Project

Figure 12 depicts the powerhouse cavern including the surge and pressure shafts. The cavern consists of two major openings, i.e.,

Table 2: Material Parameters for the Three Rocks

Type of Rock	Elastic, E*			Ultimate		Bonding Stress	Phase Change	Hardening		Disturbance			Mohr-Coulomb	
	$\bar{n}$	K	ν	γ	β	3R (MPa)	n	a_1	η_1	A	Z	D_u	c (MPa)	$\phi°$
Quartz Mica Schist	0.2645	28269	0.2	0.0202	0.4678	46.99	5.0	0.13E-13	0.6	220.7	1.339	0.97	6.38	22.24
Biotite Schist	0.2597	59320	0.2	0.0429	0.6431	57.54	5.0	0.5E-13	0.62	107.4	1.111	0.98	13.11	34.45
Quartz Mica Schist with Quartz Veins	0.9806	2641	0.2	0.097	0.74	4.73	5.0	0.15E-11	0.3	147.6	1.1054	0.99	6.37	44.41

*E = K E K $\bar{n}$, $_3$ = confining stress

Table 3: Material Parameters for Intact and Jointed Rock Mass (Quartz, Mica Schist)

Type	Elasticity		Ultimate		Phase Change	Hardening		Bonding Stress (MPa)	Disturbance		
	ν	E	γ	β	n	a_1	η_1	3R	D_u	A	Z
Intact Rock	0.2	8591	0.02020	0.4678	5.0	0.013E-12	0.6	46.99	0.97	220.70	1.339
Rock Mass	0.2	6677	0.01352	0.3889	5.0	0.013E-12	0.6	41.9	0.97	220.71	1.339

Table 4: Comparison of Predicted (FEM) and Observed (Instrumentation) Displacements at Boundary of Powerhouse Cavern

	Excavation Stage			Deformation (mm)	
Stage No.	From El. (m)	To El. (m)	Instrumentation at El. (m)	Predicted (FEM)	Observed (Instrumentation)
1	Widening of Central drift		1024 (A)	10.4	13-18
2	Widening of Central drift		1022 (B)	12	6-12
3	1018	1006	1022 (B)	0.6	-1.3 to +2.5
4	1006	1000	1018 (C)	3.5	1-4
5	1000	975	1006 (D)	23.7	10-45
6	983	975	996 (E)	9.4	1-3

machine (powerhouse) hall 216 m x 20 m x 49 m with the overburden of 262.5 m at the crown, and the transformer hall 198 m x 18 m x 29 m, Fig. 12. The openings are located in the left bank, about 500 m from the Satluj River. Based on the measurements and analysis, the co-efficient of lateral pressure was found to be 0.8035 for the E-W section considered here in (Varadarajan et al., 2001a; 2001b; Bhasin et al., 1996)

The National Institute of Rock Mechanics (NIRM), India, instrumented the powerhouse cavern site to measure the movements in the rock mass during various sequences of excavation (NIRM, 1997). The instrumentation included mechanical and remote extensometers. Figure 13 shows instrumentation scheme for a section in the middle of the cavern; A, B, C, D denote various instrument sets at various elevations.

The DSC model was used to characterize the behavior of the rocks. A finite element procedure, DSC-SST2D (Desai, 1997), which contains the DSC model, was used to analyze the cavern.

The rocks in the area of the powerhouse cavern (machine hall) are quartz mica schist and biotite schist (Varadarajan et al., 2001a; 2001b; Bhasin, et al., 1995). However, since the former is predominant in the vicinity of cavern, it is considered in the FE analysis. Also, the rock mass contains joints and discontinuities, with average Rock Mass Rating (RMR) and Tunnelling Quality Index (Q) are 50 and 2.7, respectively (Varadarajan et al., 2001a; 2001b). Therefore, the material parameters for the rock mass are obtained by modifying the foregoing intact rock parameters. The procedures proposed by Ramamurthy (1993) and Bhasin, et al. (1995) are used for such modifications. The model parameters for both the quartz mica schist and the jointed rock mass are presented in Table 3. As can be seen, the values of E, , and 3R for the rock mass are decreased compared to the intact rock.

The finite element mesh with boundary conditions, Fig. 14, contains 1167 nodal points and 364 eight-noded isoparametric elements. The initial stresses in the elements were obtained by using Ko = 0.8035. The primary loading is caused by the excavation, which is simulated in twelve (12) stages or sequences, Fig. 15. The computer code DSC-SST2D (Desai, 1997) was used for the analyses. For each sequence of excavation, the element and nodes to be removed were deactivated. In other words, the stiffness matrices and load vectors of the deactivated elements were not included in the global stiffness matrix and load vectors. The analysis was performed using the incremental iterative procedure (Desai et al., 1991).

Results

The FE results in terms of displacements, strains and stresses were processed through the commercial code, NISA (1993). Figure 16 shows contours of horizontal displacements around the cavern. The maximum displacement of about 42.6 mm was measured at the face of the cavern. It decreased to about 9.22 mm at the distance of 73 m from the face of the cavern. The predicted displacement by the present analysis at the face was about 43.0 mm, Fig. 14; the predictions compare very well with the measured value.

Figure 17 shows the contours for the vertical displacements. The predicted upward displacement near the top was about 24.0 mm, while near the bottom, the maximum downward displacement was abut 12.70 mm.

Table 4 shows comparison between predictions from the FE analysis and observations for displacements at the Powerhouse Cavern boundary, for stages one to six, Fig. 15. It can be seen that overall, the predictions compare very well with the measurements.

Conclusions

The behavior of geologic materials and joints play a significant role in design, construction and maintenance of underground space. The available models based on elasticity, plasticity, etc. are not capable to account for the effects of important factors that influence the material behavior. A new constitutive modeling approach called the Disturbed State Concept (DSC) has been developed that allows for the effects of most of the important factors. The mathematical framework of the model is general and unified, and allows for elastic, plastic and creep strains, stress path, volume change, microcracking leading to softening, fracture and failure, strengthening and healing, thermal and rate effects, and different types of loading. Most of the previously available models can be extracted from the DSC as special cases. One of its advantages is that it can be specialized to model joints and interfaces.

The DSC has been applied successfully to model behavior of a wide range of materials and joints; e.g., geologic (clay, sand, glacial till), rocks, concrete, asphalt concrete metal and alloys, rock joints and interfaces in

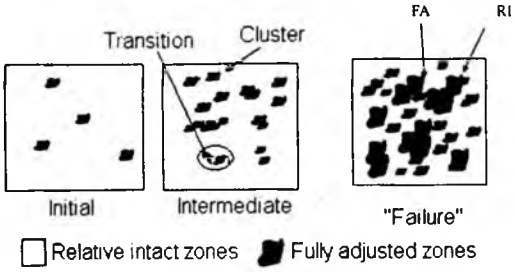

Fig. 1. Phases in Disturbed State Concept

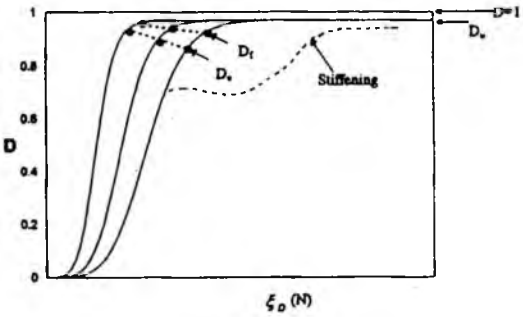

(a) Disturbance vs. Deviatoric Plastic Strain, ?D, or Loading Cycles, N

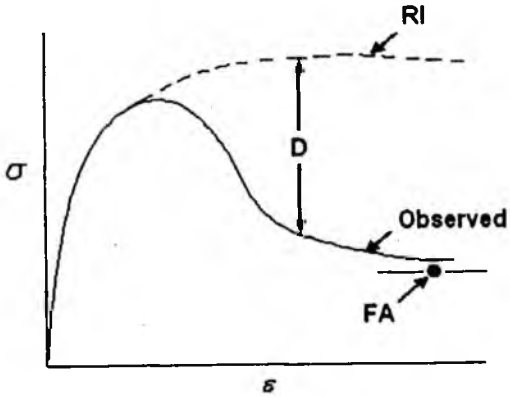

(a) Stress-strain Behavior and Disturbance, D

Fig. 2. Disturbance and Stress-strain Behavior

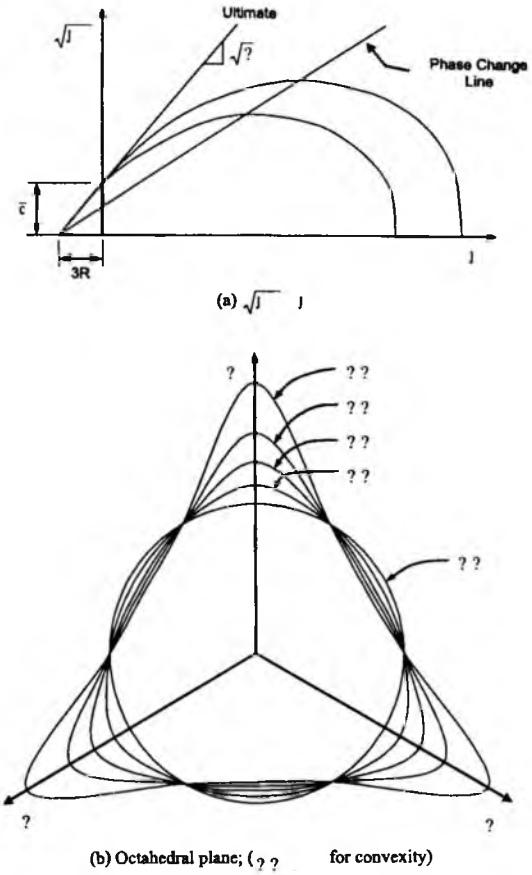

Fig. 3. Plots of Yield Surface, F, in Stress Spaces

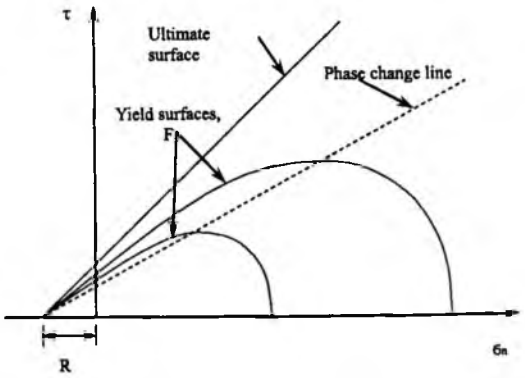

Fig. 4. HISS Yield Surfaces for Joint

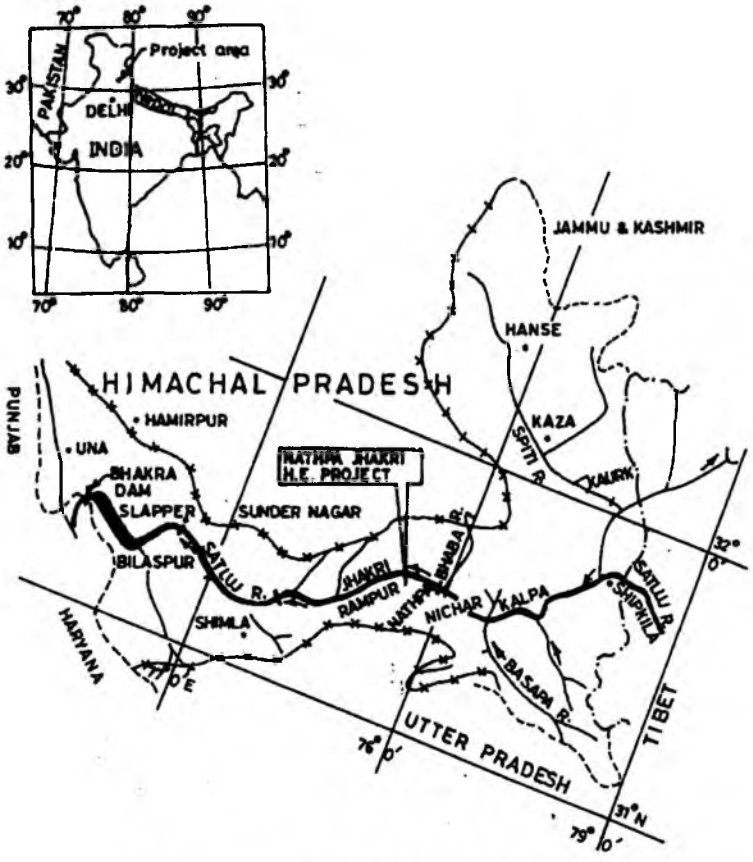

Fig. 5. Location of Nathpa-Jhakri Project Site

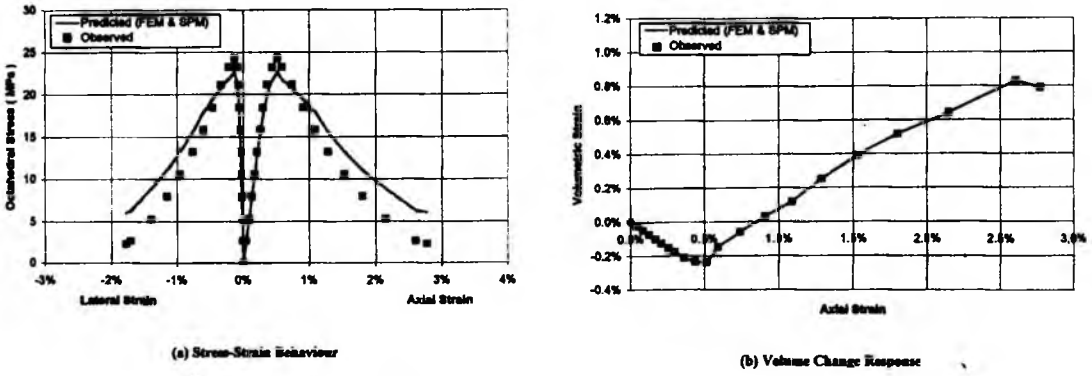

(a) Stress-Strain Behaviour

(b) Volume Change Response

Fig. 6. Stress-strain-volume Change Response and Predictions for Quartz Mica Schist, 3=30 MPa

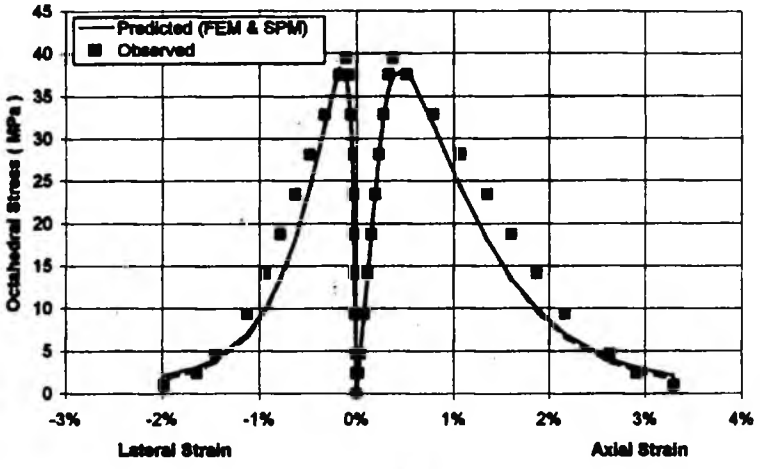

(a) Stress-Strain Behaviour

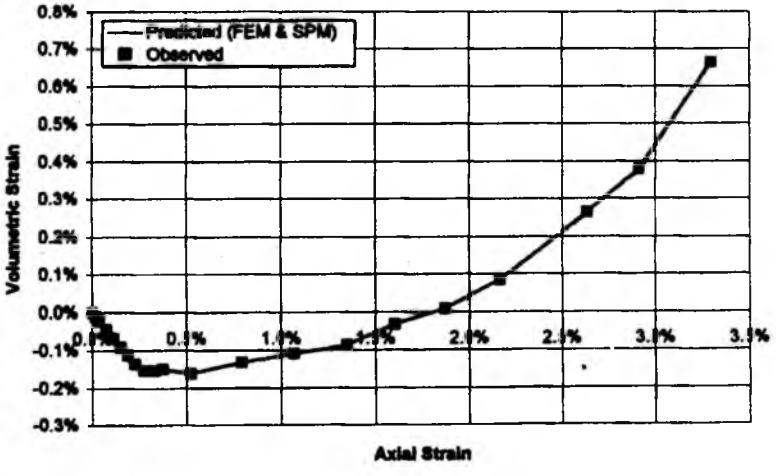

(b) Volume Change Response

Fig. 7. Stress-strain-volume Responses and Predictions for Quartz Mica Schist with Quartz Veins, ?3 = 10 MPa

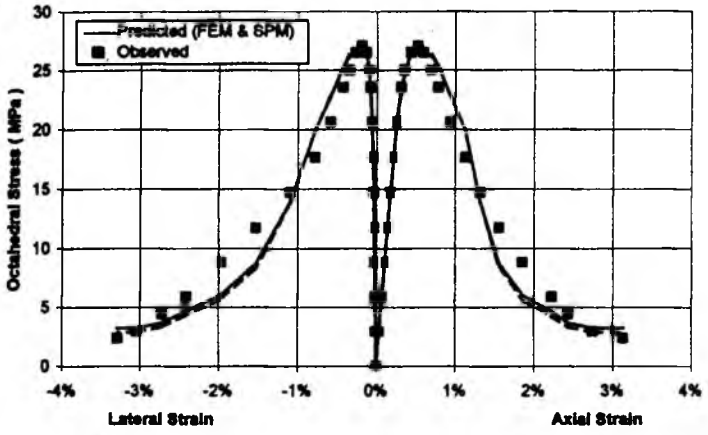

(a) Stress-Strain Behaviour

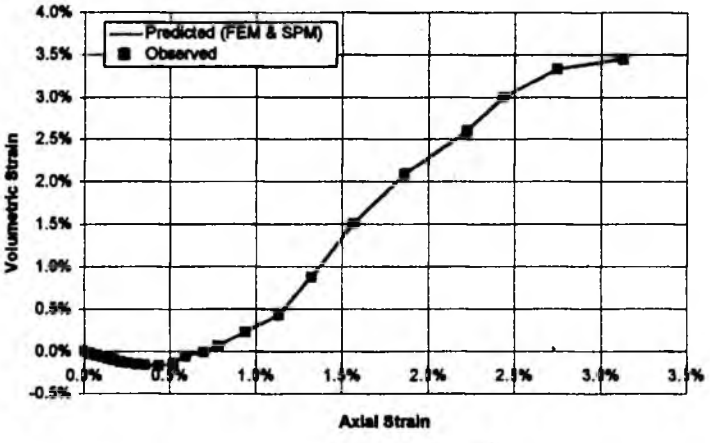

(b) Volume Change Response

Fig. 8. Stress-strain -volume Change Responses and Predictions for Biotite Schist, 3= 7.5 MPa

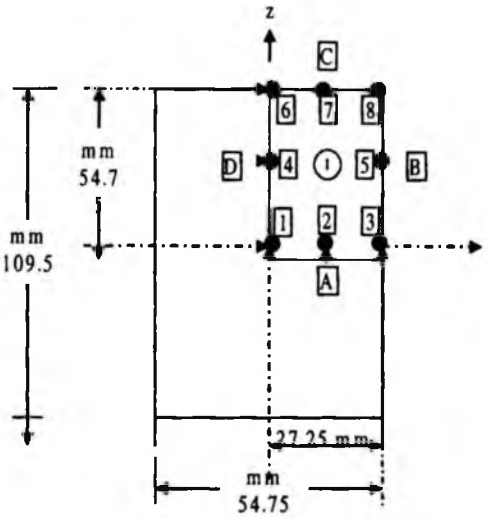

Fig. 9. Finite Element Mesh for Quarter Specimen in Triaxial Test

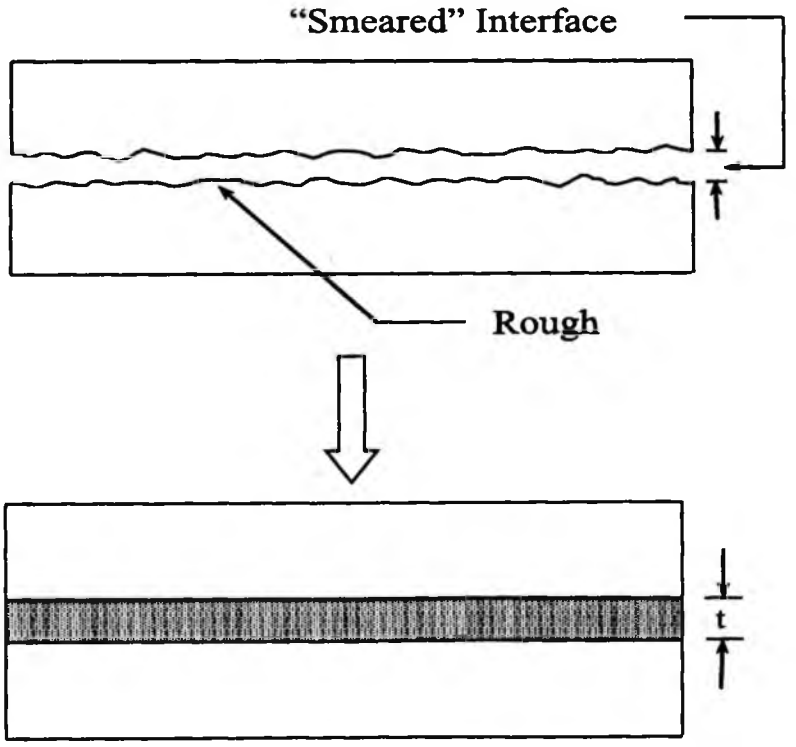

Fig. 10. Schematic of Interface Element with Thickness, t

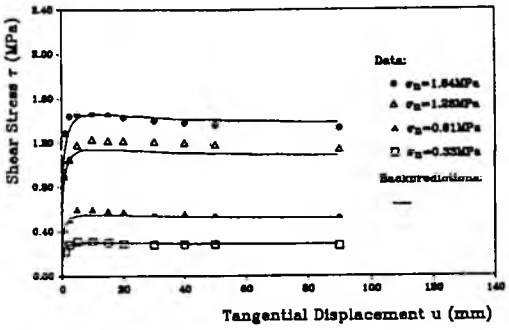

(a)

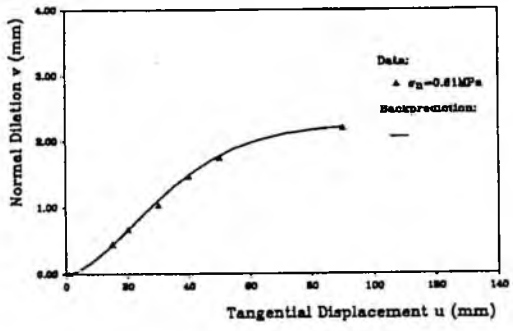

(b)

Fig. 11. Comparisons between Predictions and Observations: Type C Joint- (a) Shear Stress vs. Tangential Displacement, (b) Normal vs. Tangential Displacements

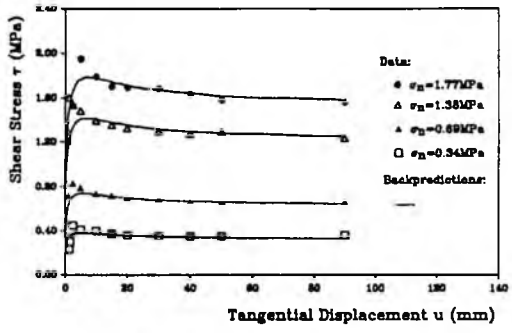

(c)

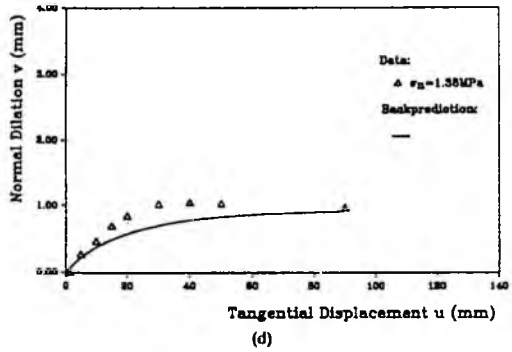

(d)

Fig. 11. (continued). Type A Joint: (c) Shear Stress vs. Tangential Displacement, (d) Normal vs. Tangential Displacements

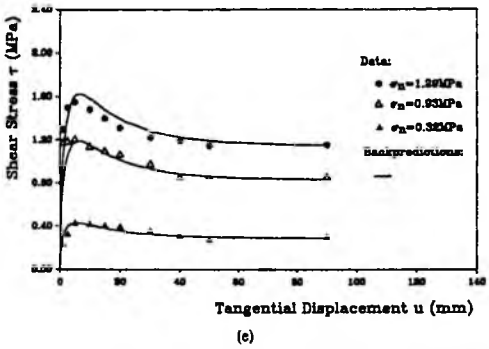

(e)

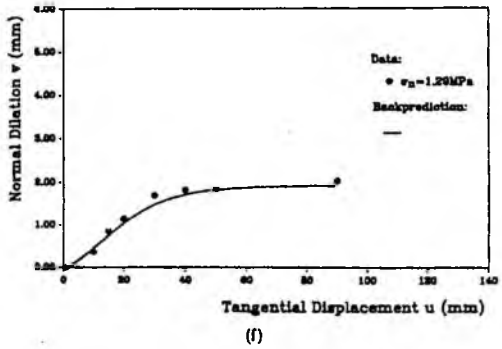

(f)

Fig. 11. Type B Joint: (e) Shear Stress vs. Tangential Displacement, (f) Normal vs. Tangential Displacements

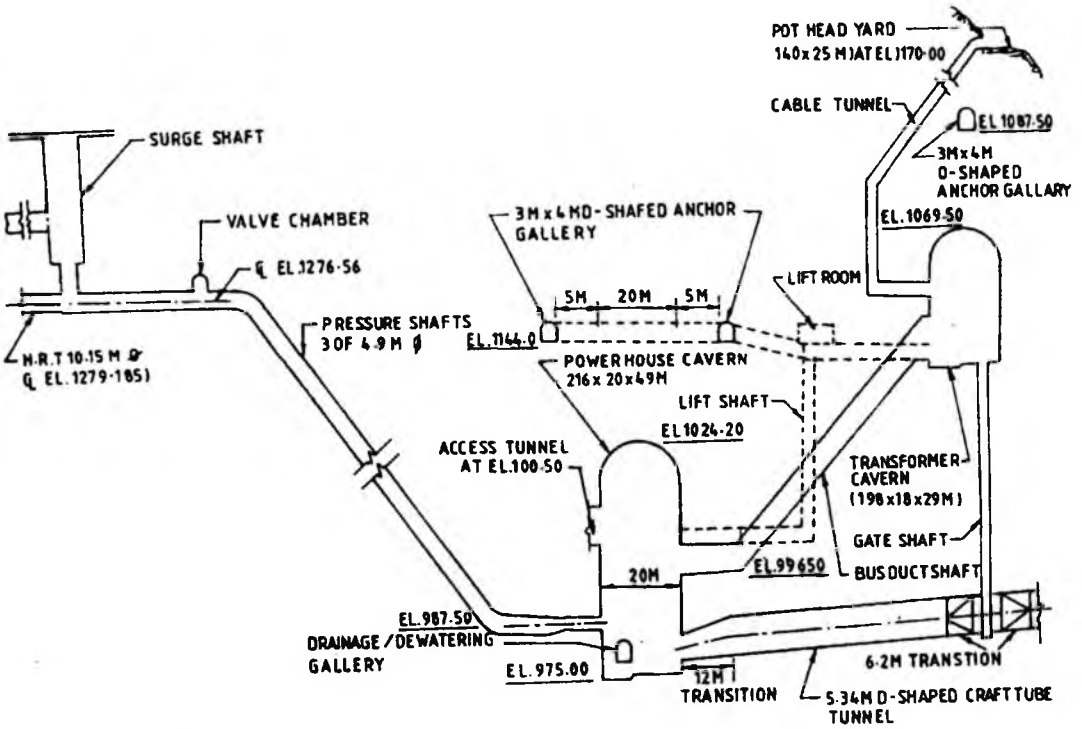

Fig. 12. East-West Section of Powerhouse Cavern, Surge and Pressure Shafts, Nathpa-Jhakri Project

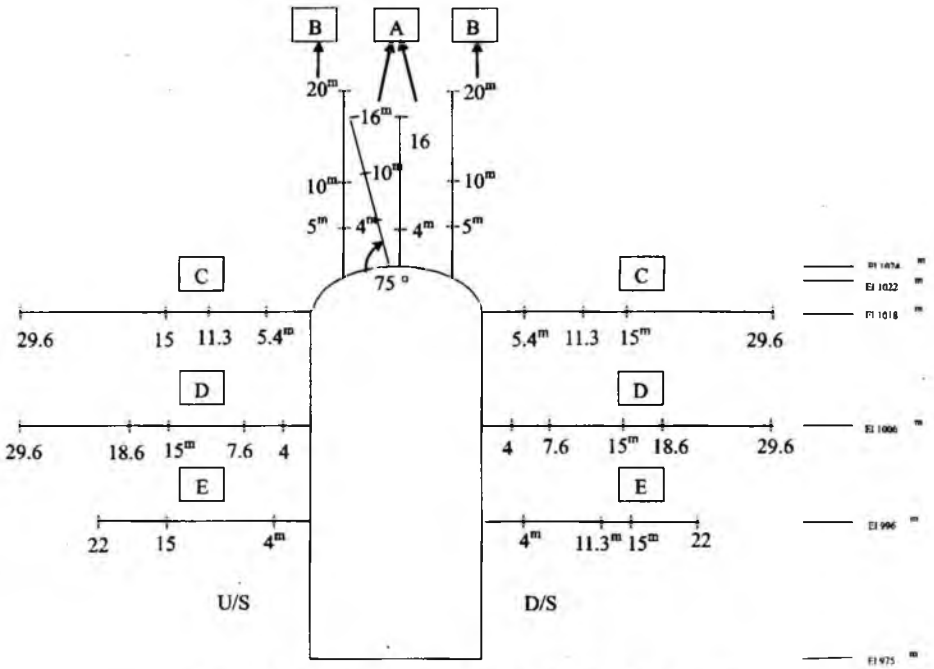

Fig. 13. Instrumentation at Mid Section of Cavern

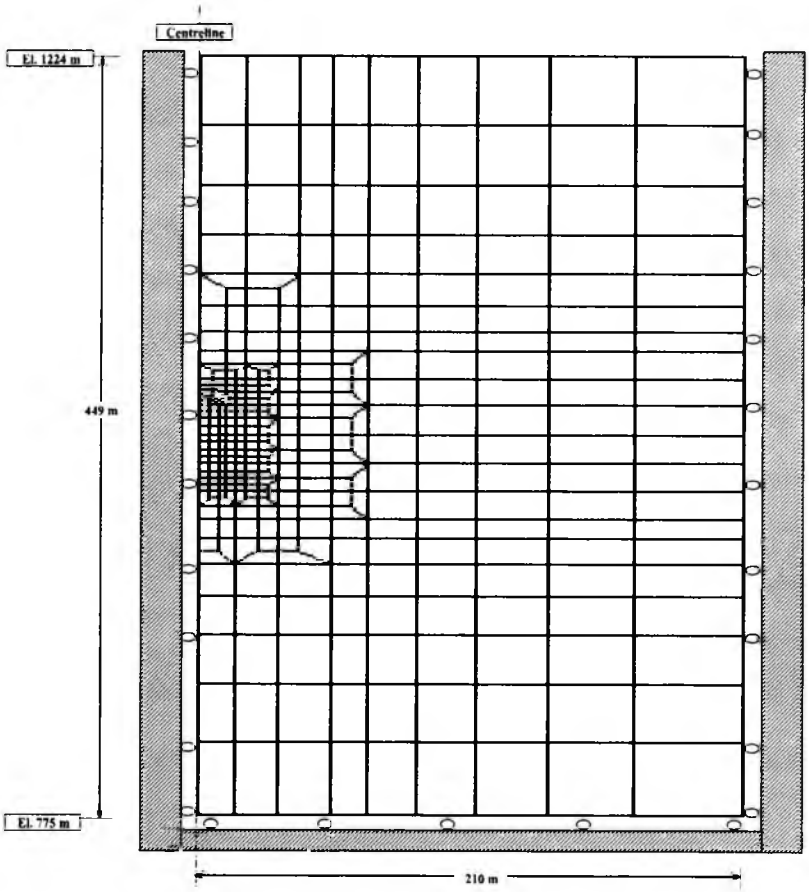

Fig. 14. Finite Element Mesh for Cavern in Rock Mass

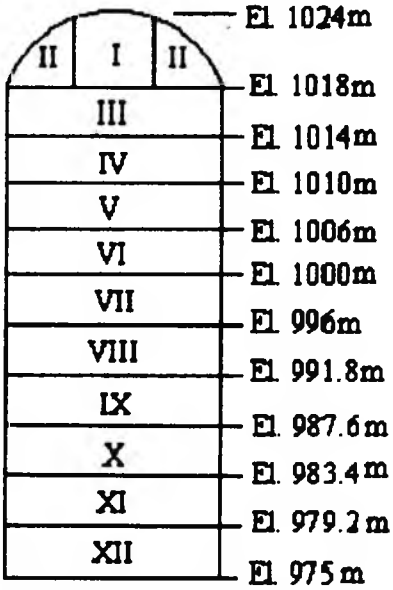

Fig. 15. Excavation Sequences for the Powerhouse Cavern

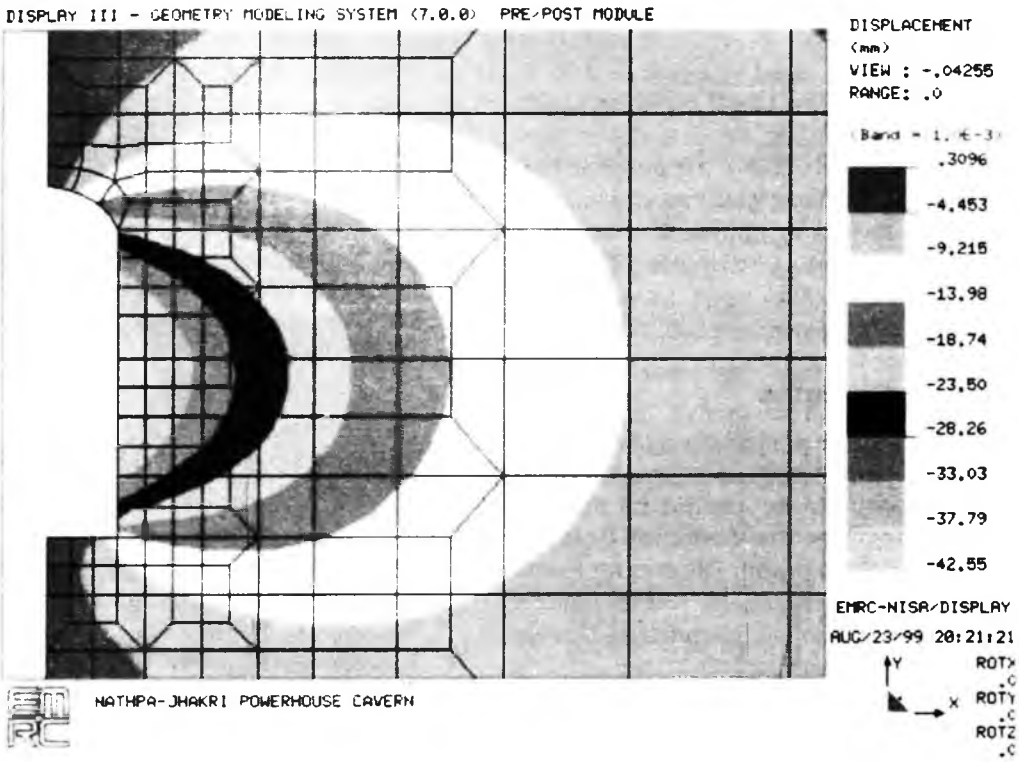

Fig. 16. Contours of Horizontal Displacements around Cavern

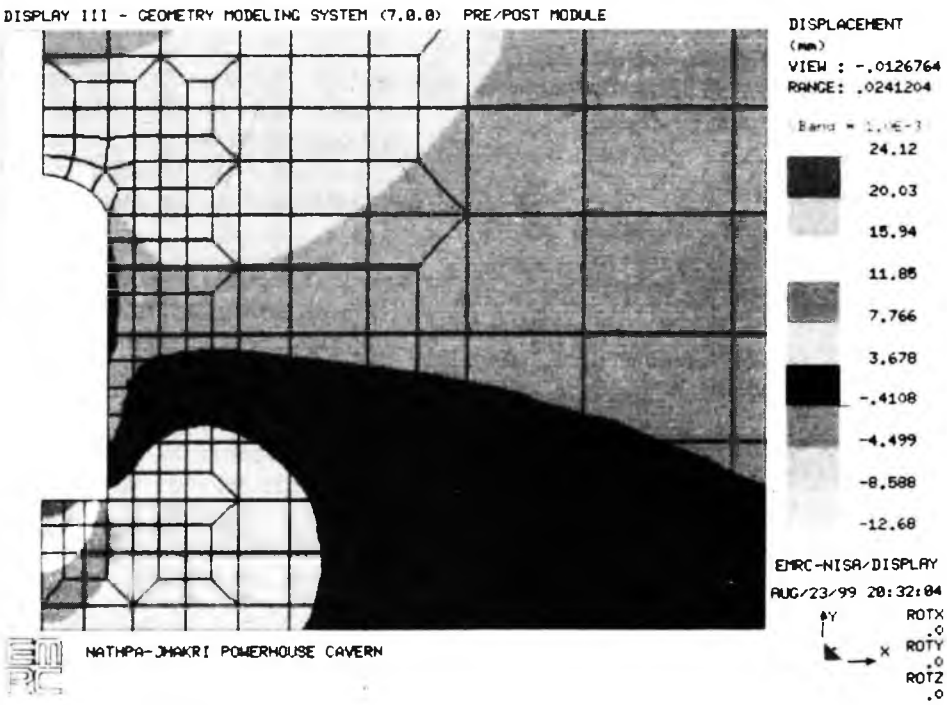

Fig. 17. Contours of Vertical Displacement around Cavern

structure and foundation problems. Finite element procedures, in which the DSC is implemented, are used to solve 2- and 3-dimensional problems under conditions such as dry, saturated, static, cyclic and repetitive loading (Desai et al., 2001). It is believed that the DSC can provide general and unique constitutive modeling approach for a wide range of materials and joints. Thus its application potential goes beyond that provided by other previously available model.

Acknowledgements

This paper includes contributions of a number of students and coworkers of the author. It has been partially supported by various organizations like the National Science Foundation, Washington, DC and Air Force Office of Scientific Research. The validations in this paper relate to the Powerhouse Cavern in the Nathpa-Jhakri hydropower project. The research for this project was supported partly by Grant Nos. Int. 9213752 and 9300828 from the International Program, National Science Foundation, Washington DC under U.S.-India Cooperative project between the Indian Institute of Technology (IIT), New Delhi, and The University of Arizona, Tucson, AZ; Drs. A. Varadarajan and K.G. Sharma acted as principal investigators at IIT-Delhi.

References

Bhasin, R., Barton, N., Grimstadt, E. and Chryssanthakis, P. (1995): "Engineering Characterization of Low Strength Anisotropic Rocks in the Himalayan Region for Assessment of Tunnel Support," *Eng. Geology,* 40, 169-193.

Bhasin, R.K., Barton, N., Grimstad, E., Chryssanthakis, P. and Shende, E.P. (1996): "Comparison of Predicted and Measured Performance of a Large Cavern in the Himalayas," *Int. J. Rock Mech. Sci., Geomechanics Abstr.,* 33, 6, 607-626.

Desai, C.S. (1997): "DSC-SST2D: Computer Code for Stratic and Dynamic-Solid, Structure and Soil-Structure Analysis," Tucson, Arizona.

Desai, C.S. (2001): *Mechanics of Materials and Interfaces: The Disturbed State Concept,* CRC Press, Boca Raton, FL, USA.

Desai, C.S. and Hashemi, Q.S.E. (1989): "Analysis, Evaluation and Implementation of a Nonassociative Model for Geologic Media," *Int. J. Plasticity,* 5, 397-420.

Desai, C.S. and Ma, Y. (1992): "Modelling of Joints and Interfaces Using the Disturbed State Concept," *Int. J. Num. Analyt. Methods in Geomech.,* 16, 623-653.

Desai, C.S. and Toth, J. (1996): "Disturbed State Constitutive Modeling Based on Stress-Strain and Nondestructive Behavior," *Int. J. Solids Struct.,* 33, 11, 1619-1650.

Desai, C.S., Chia, J., Kundu, T. and Prince, J.L. (1997): "Thermomechanical Response of Materials and Interfaces in Electronic Packaging, Parts I & II," *J. of Elect. Packaging, ASME,* 119, 294-300, 301-309.

Desai, C.S., Sane, S. and Jensen, J. (2009): "Constitutive Modeling Including creep and Rate Dependent Behavior and Testing of Glacial Tills for Prediction of Motion of Glaciers," *Int. J. of Geomechanics, ASCE,* Accepted for Publication.

Desai, C.S., Sharma, K.G., Wathugala, G.W. and Rigby, D.B. (1991): "Implementation of Hierarchical Single Surface 0 and 1 Models in Finite Element Procedure," *Int. J. of Numer. Analyt. Meth. Geomechanics,* 15, 9, 649-680.

Desai, C.S., Somasundaram, S. and Frantziskonis, G. (1986): "A Hierarchical Approach for Constitutive Modeling of Geologic Materials," *Int. J. Num. Anal. Methods in Geomech.,* 10, 3, 225-257.

Desai, C.S., Zaman, M.M., Lightner, J.G. and Siriwardane, H.J. (1984): "Thin-Layer Element for Interfaces and Joints," *Int. J. Num. and Analyt. Methods in Geomechanics,* 8, 1, 19-43.

DiMaggio, F.L. and Sandler, I. (1971) "Material Model for Granular Soils," *J. Eng. Mech., ASCE,* 97, 3, 935-956.

Goodman, R.E., Taylor, R.L. and Brekke, T.L. (1968): "A Model for the Mechanics of Jointed Rock," *J. of Soil Mech. and Found. Eng., ASCE,* 94, 637-659.

Kachanov, L.M. (1986): *Introduction to Continuum Damage Mechanics,* Martinus Nijhoft Dorchrecht, The Netherlands.

Mühlhaus, H.B. (Editor) (1995): *Continuum Models for Materials and Microstructure,* John Wiley, Chichester, UK.

National Institute of Rock Mechanics (1997): "Rock Mechanics Instrumentation to Evaluate the Long-Term Stability of Powerhouse, Kolar Gold Fields, Karnatake, India," NIRM.

NISA (1993): "User's Manual for NISA," Engineering Mechanics Research Corporation, Detroit, MI.

Ramamurthy, T. (1993): "Strength and Modulus Responses of Anisotropic Rock," Chap. *13* in *Comprehensive Rock Engineering,* Vol. 1, Pergamon Press, Oxford, UK.

Roscoe, A.N., Schofield, A., and Wroth, P.C. (1958): "On Yielding of Soils," *Geotechnique,* 8, 22-53.

Schneider, H.J. (1976): "The Friction and Deformation Behavior of Rock Joint," *Rock Mech.,* 8, 169-184.

Somasundaram, S. and Desai, C.S.(1988): "Modelling and Testing for Anisotropic Behavior of Soils," *J. Eng. Mech., ASCE,* 114, 1473-1496.

Varadarajan, A., Sharma, K.G., Desai, C.S. and Hashemi, M. (2001a): "Constitutive Modeling of Schistose Rock in the Himalaya," *Int. J. Geomechanics, ASCE,* 1, 1, 83-107.

Varadarajan, A., Sharma, K.G., Desai, C.S. and Hashemi, M. (2001b): "Analysis of a Powerhouse Cavern in the Himalaya," *Int. J. Geomechnics, ASCE,* 1, 1, 109-127.